Structural Mapping of the ϵ-Subunit of Mitochondrial H^+-ATPase Complex (F_1)

Edi Gabellieri,* Giovanni B. Strambini,* Alessandra Baracca,# and Giancarlo Solaini§
*Consiglio Nazionale delle Richerche, Istituto di Biofisica, 56127 Pisa, Italy, #Dipartimento di Biochimica "G. Moruzzi," Università di Bologna, 40126 Bologna, Italy, and §Scuola Superiore di Studi Universitari e di Perfezionamento S. Anna, 56127 Pisa, Italy

ABSTRACT Phosphorescence and fluorescence energy transfer measurements have been used to locate the ϵ-subunit within the known structural frame of the mitochondrial soluble part of F-type H^+-ATPase complex (F_1). The fluorescence probe 2′-*O*-(trinitrophenyl)adenosine-5′-triphosphate was bound to the nucleotide binding sites of the enzyme, whereas the probe 7-diethylamino-3′-(4′-maleimidylphenyl)-4-methylcoumarin was attached to the single sulfhydryl residue of isolated oligomycin sensitivity-conferring protein (OSCP), which was then reconstituted with F_1. Fluorescence and phosphorescence resonance energy transfer yields from the lone tryptophan residue of F_1 present in the ϵ-polypeptide and the fluorescence labels attached to the F_1 complex established that tryptophan is separated by 3.7 nm from Cys-118 of OSCP in the reconstituted OSCP-F_1 complex, by 4.9 nm from its closest catalytic site and by more than 6.4 nm from the two other catalytic sites, including the lowest affinity ATP site. These separations together with the crystallographic coordinates of the F_1 complex (Abrahams, J. P., A. G. W. Leslie, R. Lutter, and J. E. Walker. 1994. Structure at 2.8 Å resolution of F_1-ATPase from bovine heart mitochondria. *Nature.* 370:621–628) place the ϵ-subunit in the stem region of the F_1 molecule in a unique asymmetrical position relative to the catalytic sites of the enzyme.

INTRODUCTION

The F_1F_0-ATPase (ATP synthase) of energy-coupling membranes is the enzyme responsible for the synthesis of ATP from ADP and inorganic phosphate. The reaction is driven by the electrochemical potential of protons established across the membrane by photo or respiratory oxidative processes. Homologous ATP synthase complexes are located in the inner membrane of mitochondria, thylakoyd membrane of chloroplasts, and plasma membrane of bacteria. These multisubunit complexes are composed of two sectors: F_0 and F_1. F_0 is the membrane-embedded part and is capable of proton transport, whereas F_1 is the water-exposed, hydrophilic, catalytic sector (for reviews, see Boyer, 1993; Senior, 1988; Penefsky and Cross, 1991; Capaldi, 1995). A stalk 4–5 nm long, first evidenced by Fernàndez-Moràn (1962), joins these two lobes and is involved in the energy transmission from F_0 to F_1, probably through long-range conformational changes induced by proton transport (Boyer, 1989). The stalk contains several subunits, mostly components of F_0, among which are subunit b and, in mitochondrial ATP synthase, the oligomycin sensitivity-conferring protein (OSCP). Isolated OSCP is capable of forming a stable binary complex with F_1 (Dupuis et al., 1985; Collinson et al., 1994). The F_1 sectors of all known species contain five different subunits with the stoichiometry of $\alpha_3\beta_3\gamma\delta\epsilon$ in order of decreasing molecular weight (Walker et al., 1985). However, the only α, β, and γ from the different species are homologous, whereas the δ from *Escherichia coli* corresponds to the mitochondrial OSCP, ϵ from *E. coli* corresponds to the mitochondrial δ subunit, and finally, the ϵ of mitochondria has no counterpart in subunits from other species (Walker et al., 1985). Recent crystallographic structures of the mitochondrial enzyme up to 0.28 nm resolution (Abrahams et al., 1993; Abrahams et al., 1994; Bianchet et al., 1991) have shown that the α- and β-subunits are arranged alternately in a roughly spherical agglomerate with a central cavity occupied in large part by the rod-shaped γ-subunit. F_1 contains six nucleotide binding sites at the interface between α- and β-subunits, of which only three are considered catalytic in nature (Cross and Nalin, 1982; Issartel et al., 1986). The catalytic sites display differential affinity for Mg-coordinated adenine nucleotides (Gresser et al., 1982; Weber et al., 1993), an asymmetry in structure possibly associated with the asymmetric positioning of the γ-subunit relative to the $\alpha_3\beta_3$ subassembly. The crystal structure could not show the location of the smaller δ- and ϵ-subunits, because these might be substoichiometric in the crystal. However, an increased local variation of the electron density suggested that the two subunits are probably in the stem region of F_1. The functions of these subunits are also largely unknown, but because in other sources there is evidence placing them in the stalk region joining the two lobes of ATP synthase, it is commonly believed that they play a role in signal transduction from F_0 to F_1.

Received for publication 7 October 1996 and in final form 24 January 1997.

Address reprint requests to Giancarlo Solaini, Scuola Superiore di Studi Universitari e di Perfezionamento S. Anna, via G. Carducci 40, 56127 Pisa, Italy. Tel.: 39-50-88-33-20; Fax: 39-50-88-32-15, E-mail: gsolaini@sssup.it.

The abbreviations used are: F_1, soluble part of F-type H^+-ATPases (ATP synthases); F_0, membrane sector of ATP synthase; OSCP, oligomycin sensitivity-conferring protein; CPM, 7-diethylamino-3-(4′-maleimidylphenyl)-4-methylcoumarin; TNP-ATP, 2′-*O*-(trinitrophenyl)adenosine-5′-triphosphate; MOPS, 4-morpholinepropanesulfonic acid; SDS, sodium dodecyl sulfate.

0006-3495/97/04/1818/10 $2.00

The ambiguity in the location of the ϵ-subunit within mitochondrial F_1 prompted us to investigate proximity relationships with other components of the multisubunit assembly by the method of resonance energy transfer, a method that proved to be successful in determining the distance between several specific sites in the chloroplast coupling factor (chloroplast F_1) selectively labeled with fluorescence probes (reviewed in McCarty and Hammes, 1987). Unlike chloroplast F_1, the ϵ-subunit of the mitochondrial enzyme possesses no reactive side chain that could be labeled with fluorescence probes. However, in the latter case, advantage is taken of the fact that F_1 contains a single Trp residue (Trp-4), and this probe is located in the ϵ-subunit. Fluorescence and phosphorescence energy transfer from this intrinsic chromophore are exploited to obtain distance relationships between the ϵ-subunits and fluorescence labels bound to either the nucleotide binding sites or to the OSCP peptide complexed to F_1. In the first case the acceptor chromophore is 2′-*O*-(trinitrophenyl)adenosine-5′-triphosphate (TNP-ATP), whereas in the second case it is 7-diethylamino-3-(4′-maleimidylphenyl)-4-methylcoumarin (CPM) linked to Cys-118 of recombinant OSCP. The distances derived from energy transfer experiments strongly suggest that the ϵ-subunit is indeed in the stem region of the complex placed asymmetrically with respect to the catalytic nucleotide binding sites.

MATERIALS AND METHODS

The fluorescent sulfhydryl reagent (CPM) and the fluorescent nucleotide analogue (TNP-ATP) used in the present work were purchased from Molecular Probes (Eugene, OR). ATP, phosphoenolpyruvate, Hepes, Tris, reduced nicotinamide-adenine dinucleotide, pyruvate kinase, and lactate dehydrogenase in glycerol-containing buffer were obtained from Sigma Chemical Co. (St. Louis, MO). Diethylaminoethyl-Sephadex A-50, blue Sepharose CL-6B, Sephadex G-50, Sephacryl S-300, and standard marker proteins were obtained from Pharmacia Biotech Inc. (Uppsala, Sweden).

Enzyme preparation

F_1 was extracted from sonicated beef heart submitochondrial particles and purified by diethylaminoethyl-Sephadex A-50 ion exchange chromatography according to the method of Penefsky (1975). To remove from the F_1 preparation any contaminant, the enzyme was further chromatographed first on blue Sepharose CL-6B and then on Sephacryl S-300 as recently described (Baracca et al., 1995). The enzyme solution was stored at 5°C as a suspension at 60% ammonium sulfate saturation in the presence of 4 mM ATP (pH 8); the enzyme activity was stable for several weeks in this state. The F_1 preparation to be used was obtained daily from the above suspension by centrifugation. Essentially, the sedimented enzyme was dissolved at 4–6 μM in a buffer containing 150 mM sucrose, 1 mM KH_2PO_4, 1 mM $MgSO_4$, and 10 mM K^+-Hepes (pH 8); it was desalted on a Sephadex G-50 centrifuge column (Penefsky, 1975) equilibrated with the same buffer.

Preparation of the OSCP-CPM/F_1 complex

The recombinant OSCP was a generous gift from Dr. J. E. Walker and M. J. van Raaij (Medical Research Council, Laboratory of Molecular Biology, Cambridge, UK). The OSCP labeling was performed by incubating the polypeptide (180 μM) with a fivefold excess of CPM (900 μM) in 20 mM MOPS (pH 7) for 15 h at 4°C in the dark. Unreacted probe was separated from the labeled protein by filtration and centrifugation through a Sephadex G-50 column equilibrated in 20 mM MOPS and 100 mM KCl (pH 7) (Duszynsky et al., 1988). The OSCP-CPM/F_1 complex was prepared according to a modified procedure of Dupuis et al. (1985). The OSCP-CPM adduct (30 μM) was incubated with F_1 (6 μM) in 0.5 mM EDTA, 15 mM $KHSO_4$, 0.02% Tween 20, 0.2–0.4 mM ATP, and 20 mM MOPS (pH 7) for 30 min at room temperature. The excess OSCP-CPM was separated from the OSCP-CPM/F_1 complex by ultrafiltration on Centricon 100 (Amicon). The complex comprising the label had the polypeptide composition shown in Fig. 1 as resolved by SDS-gel electrophoresis. It had an OSCP-CPM:F_1 molar ratio of 1:1 as evaluated both by scanning the gel density as reported previously (Baracca et al., 1995) and according to the method of Duszynsky et al., (1988) calculating the ratio between the probe concentration, evaluated spectrophotometrically, and the protein concentration. The OSCP-CPM/F_1 preserved the functional properties of the OSCP/F_1 complex according to the following two criteria (Collinson et al., 1994; Duszynsky et al., 1988): 1) the inactivation by exposure to cold of the OSCP-CPM/F_1 complex was lower than that of the sole F_1; and 2) the reconstituted F_1F_0 complex resulting by the addition of both F_1- and

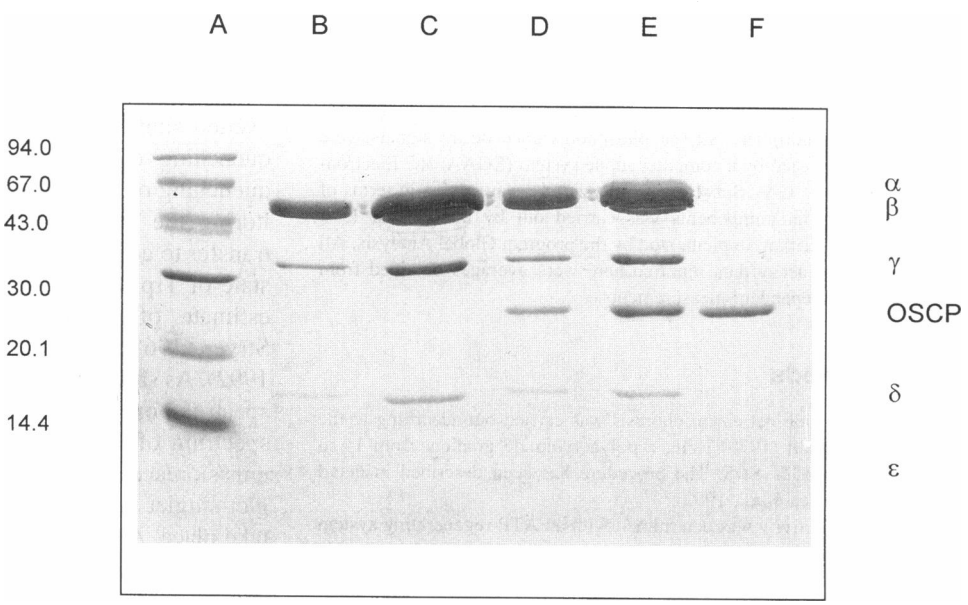

FIGURE 1 Polypeptide composition of the OSCP-CPM/F_1 complex. Lane A, molecular size marker proteins (Pharmacia): rabbit muscle phosphorylase b (94.0 kDa), bovine serum albumin (67.0 kDa), egg white ovalbumin (43.0 kDa), bovine erythrocyte carbonic anhydrase (30.0 kDa), soybean trypsin inhibitor (20.1 kDa), and bovine milk α-lactalbumin (14.4 kDa); lanes B and C, 10 and 50 μg F_1, respectively; lanes D and E, 15 and 35 μg OSCP-CPM/F_1, respectively; lane F, 2 μg OSCP. The positions of the F_1 subunits are indicated at the right.

OSCP-depleted submitochondrial particles (Tzagoloff et al., 1968) with F_1 proved to be oligomycin sensitive when the reconstitution was performed in the presence of OSCP-CPM (not shown). Incidentally, it has to be noted that the activity of both isolated F_1 and OSCP-CPM/F_1 in 50% (v/v) glycerol was unaffected after the solution had been taken to 180 K during the time required for energy transfer measurements (nearly 1 h for each sample).

Binding of TNP-ATP to F_1

Binding the nucleotide derivative TNP-ATP to F_1 was conducted according to the procedure of Grubmeyer and Penefsky (1981) modified to take into account that the study of energy transfer has to be performed at low temperature in buffer containing 50% (v/v) glycerol. The binding of TNP-ATP to F_1 was evaluated by exploiting the enhancement of fluorescence emission of TNP-ATP at 550 nm (λ_{ex} = 436 nm) when it binds to F_1 (Grubmeyer and Penefsky, 1981; Tiedge and Schäfer, 1986). Analysis of the fluorescence enhancement as a function of TNP-ATP concentration (0.01–50 μM), taking into account different factors for fluorescence enhancement due to the occupation of different sites (Tiedge and Schäfer, 1986), yields nearly three (2.7 $\pm$ 0.15) binding sites: one of high affinity, of which it was not possible to calculate the K_D, and two of lower affinity, exhibiting K_D values of 0.34 and 0.48 μM (at 22°C), values slightly higher than those reported in the absence of glycerol by other groups (Murataliev and Boyer, 1994; Muneyuki et al., 1994; Weber and Senior, 1996). To test the possible effects of low temperature on K_D, the binding isotherm was also repeated at 5°C. At this temperature, the K_D values for the lower affinity sites increased to 0.40 and 0.67 μM, indicating a significant loss in affinity at lower temperatures. When 1 mM Mg-ATP was added to the F_1 solution containing TNP-ATP, the amplitude of the fluorescence enhancement decreased, reaching the amplitude corresponding to that observed for the 1:1 F_1:TNP-ATP molar ratio. This confirms a very tight binding of the nucleotide derivative to its highest affinity binding site. It should be noted that the highest affinity TNP-ATP site corresponds to the lowest affinity catalytic site for ATP (Murataliev and Boyer, 1994). For this reason, the labeled nucleotide that is tightly bound to F_1 is not displaced by Mg-ATP.

Fluorescence and phosphorescence measurements

A conventional homemade instrument was used for all fluorescence and phosphorescence intensity and decay measurements (Cioni and Strambini, 1989). The samples were placed in cylindrical spectrosil cuvettes (4 mm inside diameter). Continuous excitation, provided by a Cermax xenon lamp (LX 150UV; ILC Technology, Sunnyvale, CA), was selected by a 0.25-m grating monochromator with a 10-nm bandpass. The emission collected through another 0.25-m grating monochromator (H25; Jobin-Yvon, Longjumeau, France) with a 3-mm bandwidth, was detected with an EMI 9635 QB photomultiplier. All the phosphorescence decay signals were digitized and averaged by a computer scope system (EGAA; RC Electronics, Santa Barbara, CA). Subsequent analysis of decay curves in terms of discrete exponential components was carried out by a nonlinear least square fitting algorithm, implemented by the program Global Analysis. All the intensity and decay data reported here were averages obtained from three or more independent measurements.

Other methods

SDS-polyacrylamide gel electrophoresis was carried out according to the method of Laemmli (1970) using a polyacrylamide gradient from 14 to 25% containing 0.1% SDS. The procedure has been described in detail previously (Baracca et al., 1992).

The ATPase activity was determined with an ATP-regenerating system by following the decrease of reduced nicotinamide-adenine dinucleotide absorption at 340 nm in a Jasco (Tokyo, Japan) model 7850 spectrophotometer. The assay was carried out at a substrate saturating concentration (steady state) as previously reported (Solaini et al., 1993). The specific activity of the enzyme was 80–100 units/mg protein at 20°C.

Protein concentrations of enzyme solutions were determined by the method of Lowry et al. (1951).

RESULTS

Fluorescence and phosphorescence resonance energy transfer from Trp of the ϵ-subunit to coumarin-labeled OSCP bound to F_1

Förster type singlet-singlet fluorescence energy transfer from the lone Trp residue (donor) of the ϵ-subunit of F_1 and the coumarin (CPM) probe (acceptor) attached to OSCP entails a decrease in both the fluorescence yield and lifetime of the donor as well as an enhancement of the fluorescence yield of the acceptor. Unfortunately, direct quantitative measurements of the transfer efficiency from the extent of donor fluorescence quenching or acceptor fluorescence sensitization turned out to be problematic with the F_1 complex. The reason is that in the F_1 oligomer, there are nearly 100 Tyr residues (Walker et al., 1985) to 1 Trp residue, and selective detection of Trp fluorescence is virtually impossible, especially if one or more Tyr is in the ionized state. This supposition was confirmed by the phosphorescence spectrum of F_1 in that it shows a distinct Tyr contribution (Fig. 2, $\lambda_{em} \leq 400$ nm) even when the sample is excited at the red edge of Trp absorption (295 nm). For the same reason, the extent of sensitization of coumarin fluorescence cannot be used to derive the transfer efficiency from Trp, because any excited Tyr could also take part in the sensitization process. In addition to these difficulties, the large size of F_1 causes considerable scattering of the excitation, and the relatively weak fluorescence signal is partly submerged by a relatively high scattering background.

These difficulties in quantifying the extent of Trp fluorescence quenching were overcome by using the phosphorescence emission of Trp in low-temperature glycerol/buffer glasses. Under these conditions the phosphorescence spectrum of Trp is clearly distinguishable from that of Tyr in that it is shifted about 50 nm to the red and exhibits a pronounced vibronic structure (Fig. 2, *A* and *B*). Because the excited singlet state is a precursor of the triplet state, any quenching of fluorescence will result in a proportional quenching of phosphorescence. Another advantage of monitoring the phosphorescence is that dipole-dipole energy transfer to coumarin is also possible from the excited triplet state of Trp, thus providing an additional and independent estimate of donor-acceptor separation (Kellogg, 1967; Stryer, 1968; Galley and Stryer, 1969; Strambini et al., 1992). As shown in Fig. 3, *A* and *B*, the coumarin absorption spectrum overlaps the fluorescence and phosphorescence spectrum of Trp and thus satisfies the requisite of donor-emission/acceptor-absorption spectral overlap for both singlet-singlet and triplet-singlet resonance energy transfer to take place. Although both singlet and triplet energy transfer cause a reduction of the phosphorescence intensity, the extent of quenching by the latter process can be distin-

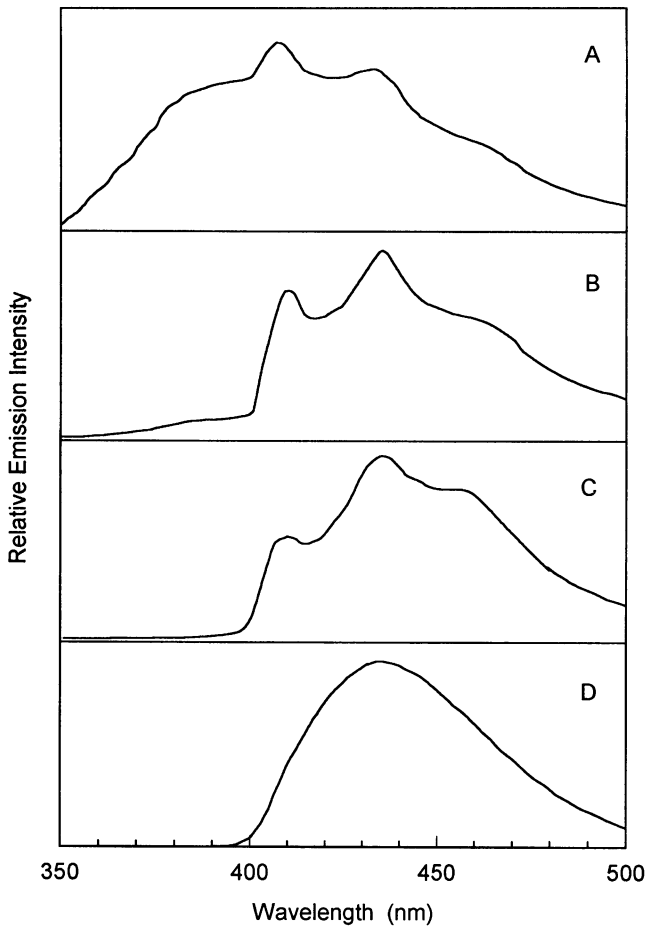

FIGURE 2 Phosphorescence spectra of F_1 from beef heart mitochondria (*A*, λ_{ex} = 280 nm; *B*, λ_{ex} = 295 nm) and of the OSCP-CPM/F_1 complex (*C*, λ_{ex} = 295 nm). (*D*) Fluorescence spectrum of OSCP-CPM (λ_{ex} = 340 nm). All samples are in glycerol/MOPS buffer (50:50, v/v) at 180 K. F_1 and OSCP-CPM/F_1 were 2.7 μM; OSCP-CPM was 15.4 μM.

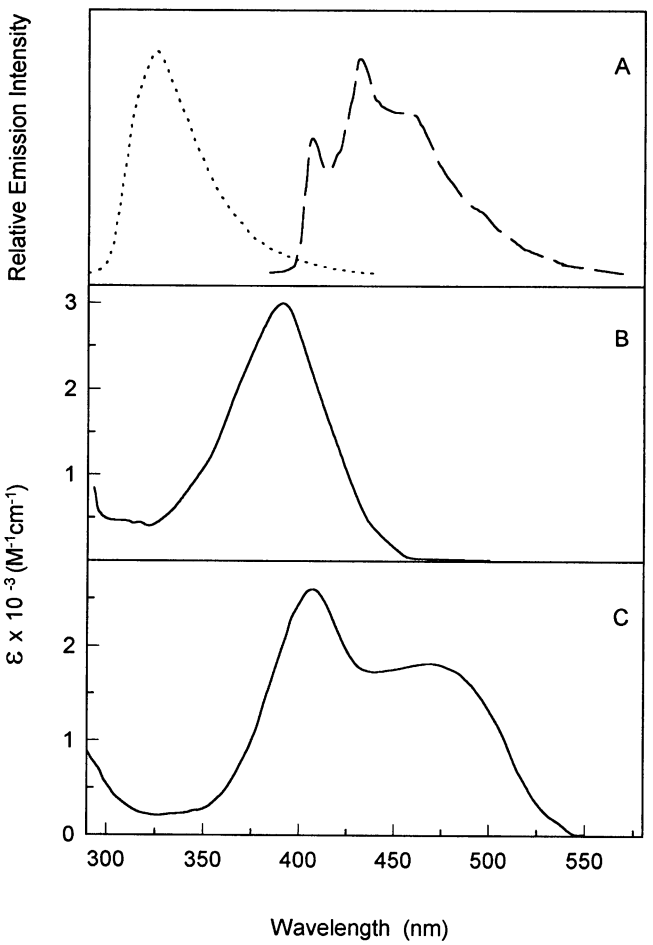

FIGURE 3 Donor-emission and acceptor-absorption spectra used in the calculation of spectral overlaps for resonance energy transfer. (*A*) Trp fluorescence (····) and phosphorescence (— — —), spectra. (*B*) OSCP-CPM absorption spectrum. (*C*) TNP-ATP absorption spectrum. The solvent was 10 mM KH_2PO_4, 2 mM $MgSO_4$, and glycerol (50:50, v/v), pH 7.4, whereas the temperatures were 180 and 293 K for emission and absorption spectra, respectively.

guished from the former, because only the latter entails a shortening of the triplet state lifetime.

The phosphorescence spectrum of F_1 in a 50:50 (v/v) glycerol/MOPS buffer glass at 180 K is shown in Fig. 2. At the excitation wavelength of 295 nm the emission is largely due to Trp, as opposed to excitation at 280 nm, in which the phosphorescence spectrum is dominated by Tyr emission (the only contributor at $\lambda \leq 400$ nm). At the excitation wavelength of 295 nm there is a residual Tyr emission, which is 10–15 nm red shifted relative to neutral Tyr, as would be expected for ionized Tyr phosphorescence. Its intensity at 411 nm, the wavelength of the Trp 0–0 vibronic band, amounts to about 7–8% of the total phosphorescence. Impurities emission from glycerol, even if the temperature of the glass was chosen to minimize this solvent background, also contributes a few percent to the overall phosphorescence intensity at this wavelength.

Formation of the OSCP-CPM/F_1 complex gives rise to a detectable reduction of the Trp phosphorescence intensity and lifetime as well as the appearance of sensitized coumarin prompt and delayed fluorescence. The magnitudes of these changes for OSCP-CPM concentrations ranging between 2.7 and 15.4 μM, or OSCP-CPM/F_1 molar ratios between 1 and 6, are given in Table 1.

The overall decrease in steady-state Trp phosphorescence intensity, P/P_0, as measured at the maximum of the 0–0 vibronic band (411 nm) and corrected for the Tyr-solvent contribution, is up to 48%. Part of this reduction, however, is to be attributed to the inner filter by the coumarin label of both the excitation light (λ = 295 nm) and the phosphorescence emission at 411 nm (trivial energy transfer). Indeed, controls with free Trp mixed with OSCP-CPM, at the various concentrations used with F_1, showed that the inner filter reduces the $P:P_0$ ratio up to 17%. After correcting for the inner filter (Table 1, values shown in parentheses), one finds that the net decrease in P/P_0 is about 30% and that it occurs entirely at an OSCP-CPM:F_1 molar ratio of 1.

The decay kinetics of Trp phosphorescence in F_1 are, as previously reported, heterogeneous. The emission collected

TABLE 1 Trp phosphorescence quenching and coumarin fluorescence sensitisation by binding of OSCP-CPM to F_1

Sample	[OSCP] / [F_1]	CPM fluorescence (λ_{em} = 445 nm) F^{295}/F^{340}	Trp phosphorescence P/P$_0$ (λ_{em} = 411 nm)	τ_1 (s)	τ_2 (s)	τ_3 (s)	f_1	f_2	f_3
F_1 (2.7 μM)			1.0	4.92	1.61	0.34	0.60	0.26	0.14
F_1 + OSCP-CPM	1.07	1.05	0.68 (0.71)	4.40	1.36	0.31	0.51	0.26	0.23
F_1 + OSCP-CPM	2.74	0.84	0.59 (0.67)	4.41	1.29	0.29	0.50	0.24	0.26
F_1 + OSCP-CPM	4.90	0.78	0.57 (0.70)	4.37	1.31	0.31	0.51	0.25	0.24
F_1 + OSCP-CPM	5.70	0.76	0.52 (0.69)	4.39	1.28	0.27	0.53	0.21	0.26
F_1 + OSCP (15.4 μM)	5.70		1.0	4.95	1.72	0.36	0.58	0.29	0.13
Trp (2.7 μM)			1.0	5.10		0.30	0.85		0.15
Trp + OSCP-CPM (15.4 μM)		0.73	0.83	4.97		0.35	0.87		0.13
OSCP-CPM (15.4 μM)		0.71							

Samples were in 50:50 (v/v) glycerol/MOPS buffer at 180 K. F^{295} and F^{340} are the coumarin fluorescence intensities obtained using λ_{ex} = 295 and 340 nm, respectively. P/P_0 refers to the phosphorescence intensity at 411 nm (λ_{ex} = 295 nm), subtracted of tyrosines and solvent contributions, relative to that of F_1. The intensity ratios (P/P_0), corrected for inner filter and trivial energy transfer are shown in parentheses. The lifetimes (τ_i) and the fractional intensities (f_i) are obtained by fitting the phosphorescence decay data with the equation: $P(t) = \Sigma f_i e^{-t/\tau i}$.

through a bandpass filter with a transmission window of 405–480 nm requires three distinct exponential components to be adequately fitted. About 14% of the intensity is short lived (τ = 0.3 s) and is believed to represent Tyr-solvent phosphorescence. Indeed, the lifetime of Tyr measured at $\lambda_{em} < 400$ nm (λ_{ex} = 280 nm; Fig. 2 *A*) is 0.2–0.3 s, which is much shorter than the 1–2.4 s that is typically observed in rigid glasses (temperature <140 K). The rest is Trp phosphorescence of which about 60% exhibits a lifetime of about 5 s, whereas for the remaining 26%, τ = 1.6 s (heterogeneity in τ reflects conformer heterogeneity of the ϵ-subunit of F_1 (Solaini et al., 1993)). At 180 K, the lifetime of 1.6 s for Trp in proteins is unusually short and probably reflects the interaction of the indole ring with some quenching amino acid side chains (Cys, Cys-Cys, His, and Tyr) in its proximity (Strambini and Gonnelli, 1995).

The association of OSCP to F_1 does not affect the triplet decay kinetics, but binding of OSCP-CPM induces a minor but distinct reduction in the Trp phosphorescence lifetime (Table 1). Once again, the effect is complete at a protein: probe molar ratio of 1. The decrease in steady-state phosphorescence intensity estimated from the shortening of τ ($P/P_0 = \Sigma_i f_i \tau_i/\tau_i^0$, f_i is the fractional intensity with unperturbed lifetime τ_i^0) is about 13%. Thus, of the overall 30% quenching of Trp phosphorescence, 17% is attributed to singlet-singlet fluorescence energy transfer and 13% to triplet-singlet phosphorescence energy transfer. The latter process is confirmed also by the observation of delayed fluorescence from the coumarin acceptor, an emission spectrally identical to prompt fluorescence but with the same long lifetime of Trp phosphorescence. Because delayed fluorescence is detected as phosphorescence it leads to an apparent distortion of the Trp phosphorescence spectrum of F_1. The phosphorescence spectrum of 1:1 OSCP-CPM:F_1, for which trivial energy transfer artifacts are negligible (Fig. 2 *C*), can indeed be reconstructed from the emission of F_1 (Fig. 2 *B*) plus a modest contribution of coumarin fluorescence (Fig. 2 *D*).

As stated above, the efficiency of Trp fluorescence resonance energy transfer can in principle also be computed from the sensitization of prompt coumarin fluorescence. Sensitization manifests itself with an increase in the fluorescence intensity ratio F^{295}/F^{340} (F^{λ}, the coumarin fluorescence intensity at 445 nm on excitation at wavelength λ) when OSCP-CPM is complexed to F_1. The enhancement is most pronounced at an OSCP-CPM:F_1 molar ratio of 1. At higher molar ratios, the magnitude of F^{295}/F^{340} decreases steadily toward the value of free OSCP-CPM as if the OSCP-CPM in excess of 1:1 contributed to the overall fluorescence ratio as would the free probe. Control experiments with free Trp in place of F_1 confirm that at the highest OSCP-CPM concentration, artifacts due to reabsorption of protein fluorescence by the coumarin probe, which would also raise the F^{295}/F^{340} ratio, are negligible.

For a donor:acceptor molar ratio of 1, the relationship between the efficiency of fluorescence energy transfer, E_T, and F^{295} (OSCP-CPM/F1)/F^{295} (OSCP-CPM) is:

$$E_T = a^{295}(\text{OSCP-CPM}) \cdot [F^{295}(\text{OSCP-CPM/F1})/F^{295}(\text{OSCP-CPM}) - 1]/a^{295}(\text{Trp})$$

(Lakowicz, 1983), where a is the molar absorptivity coefficient at the indicated wavelength. Taking a^{295} (Trp) = 3400 cm^{-1} M^{-1} for the Trp residue of F_1 and a^{295} (OSCP-CPM) = 5100 cm^{-1} M^{-1}, we obtain E_T = 0.72. This transfer efficiency is almost four times as large as that estimated from the quenching of Trp phosphorescence. The discrepancy implies that, to a large extent, coumarin sensitization is due to additional energy transfer, probably from red-absorbing tyrosinate residues. The observation of a decrease in Tyr phosphorescence intensity on binding of OSCP-CPM (Fig. 2, *B* and *C*) supports this hypothesis.

According to the theory of Förster (1959), the efficiency of singlet-singlet and triplet-singlet energy transfer is related to the distance, r, between Trp in the ϵ-subunit and the coumarin label attached to OSCP, by

$$E_T = R_0^6/(R_0^6 + r^6)$$

where R_0 is the distance for 50% energy transfer. The distances calculated from fluorescence and phosphores-

cence energy transfer yields assuming a random and fixed donor-acceptor orientation (Table 2) are 3.7 and 3.8 nm, respectively. Alternatively, distances may be estimated from the rates, k_T, [$k_T = (R_0/r)^6/\tau_0$] of triplet-singlet energy transfer derived from the shortening of the triplet lifetime components, ($k_T = 1/\tau - 1/\tau_0$). The distances calculated from the reduction of the 4.9- and 1.6-s components are 3.9 and 3.5 nm, respectively. Of course, discrepancies in r between the conformers of the ϵ-polypeptide with different Trp lifetimes (1.6 and 4.9 s) may result from a combined change of distance and average orientation. The agreement in the distances determined by fluorescence and phosphorescence energy transfer is quite good if one considers the uncertainties associated with the correction for inner filter effects and the assumption of randomized donor and acceptor orientations.

Phosphorescence resonance energy transfer from Trp of the ϵ-subunit of F_1 to bound TNP-ATP

TNP-ATP has been used in several laboratories to carry out studies on the catalytic mechanism of F-type ATPases (Grubmeyer and Penefsky, 1981; Murataliev and Boyer, 1994; Weber and Senior, 1996; Weber et al., 1993; Shapiro et al., 1991). From these studies, information on binding of the nucleotide derivative to nucleotide binding sites of F_1 from different sources has been obtained. It has been established that under our experimental conditions, that is, native F_1 (i.e., enzyme-containing endogenous adenine nucleotides) in the presence of Mg^{2+}, TNP-ATP binds selectively to the catalytic sites. The number of TNP-ATP molecules bound to the F_1 complex is three for the *E. coli* enzyme, slightly less than three on our mitochondrial preparations.

Fig. 3 *C* shows the absorption spectrum of the TNP probe linked to ATP. Clearly, donor-emission/acceptor-absorption spectral overlap is highly favorable with Trp phosphorescence but rather poor with Trp fluorescence. As a consequence, the overlap integral is large and the critical distance long range (R_0 = 3.9 nm) only for triplet-singlet energy transfer. For this reason, spectroscopic measurements were concerned exclusively with changes in Trp phosphorescence.

Table 3 reports phosphorescence intensity and the lifetime of the TNP-ATP/F_1 complex at various degrees of nucleotide saturation. Increasing concentrations of TNP-ATP lead to a considerable reduction in the P/P_0 (411 nm) intensity ratio. However, control experiments in which F_1 is replaced by free Trp show that inner filter of the excitation and trivial transfer of phosphorescence account for most if not all of the change (Table 3, see corrected P/P_0 in parentheses). Only at TNP-ATP concentrations greater than 25–30 μM is there a moderate decrease in P/P_0, reaching about 20 ± 3% at 60 μM. Further evidence of triplet-singlet energy transfer is provided by the shortening of the phosphorescence lifetime (Table 3). The reduction in intensity predicted from the lifetime shortening is in agreement with intensity data, and again τ decreases only at relatively large nucleotide concentrations. Significantly, both phosphorescence intensity and lifetime are promptly restored when 1 mM Mg-ATP is added to these solutions. This suggests that the sites at which TNP-ATP is weakly bound are specific for the nucleotide rather than for the TNP moiety. The average distance calculated for this transfer efficiency is 4.9 nm, whereas transfer rates yield 4.2 and 5.0 nm for the 1.6- and 4.9-s lifetime components, respectively (Table 2).

It must also be recognized that the shortening of the triplet lifetime could in principle be due to a change in conformation of the ϵ-subunit bringing Trp closer to a quenching moiety; a change elicited by TNP-ATP but not by ATP binding. Although this possibility cannot be ruled out, it seems unlikely, because in a conformational change, the lifetime heterogeneity is generally not preserved. Table 3 shows that the relative amplitude of the 1.6- and 4.9-s lifetime components remains invariant on TNP-ATP binding, and, moreover, the shortening of each component is commensurate with a similar rate of energy transfer in the two conformations of ϵ.

It should be noted that the concentration of TNP-ATP at which energy transfer is observed is sensibly larger than would be expected from the dissociation constant of the

TABLE 2 Trp fluorescence and phosphorescence energy transfer (ET) to OSCP-CPM and TNP-ATP

	J^* (M^{-1} cm^3)	$R_0^{\#}$ (nm)	$E^{\$}$ (%)	r (nm)	$K_T^{\P}$ (s^{-1})	r (nm)
OSCP-CPM (fluorescence ET)	$1.5 \cdot 10^{-14}$	2.83	17	3.7	—	—
OSCP-CPM (phosphorescence ET)	$8.8 \cdot 10^{-15}$	2.75	13	3.8	0.144	3.5
					0.024	3.9
TNP-ATP (phosphorescence ET)	$7.4 \cdot 10^{-14}$	3.93	20	4.9	0.406	4.2
					0.046	5

*J is the overlap integral: $J = \int I_d(\lambda) a_A(\lambda) \lambda^4 d\lambda / \int I_d(\lambda) d\lambda$, where a_A is the molar absorptivity coefficient of the acceptor, and I_d is the fluorescence or phosphorescence intensity of the donor. Fluorescence and phosphorescence spectra were corrected for the λ response of the instrument.

#$R_0^6 = (8.8 \cdot 10^{-25}) \kappa^2 n^{-4} \phi J$, cm^6, where the orientation factor κ^2 is assumed to be 0.476, as for fixed random orientations of the donor and acceptor transition dipole moments (Lakowicz, 1983). n = 1.4 is the refractive index of the medium; ϕ is the emission quantum yield of Trp; ϕ_F = 0.31 is the fluorescence quantum yield of F_1 at low temperature obtained by spectral integration and assuming ϕ_F = 0.20 for free Trp in water at 20°C (Eftink and Ghiron, 1976). Any Tyr contribution was neglected. $\phi_P = 0.45 = k_P \tau_P$ is the phosphorescence quantum yield estimated on the basis of a radiative rate k_P = 0.09 s^{-1} and τ_P = 5 s (Stryer, 1968).

§$E = R_0^6/(R_0^6 + r^6)$ is the efficiency of energy transfer, where r is the distance between donor and acceptor.

¶k_T is the rate of energy transfer. $k_T = (1/\tau_0)/(R_0/r)^6$, where τ_0 is the donor-unperturbed phosphorescence lifetime.

TABLE 3 Trp phosphorescence quenching by TNP-ATP bound to F_1

Sample*	[TNP-ATP] / [F_1]	Trp phosphorescence							
		P/P_0#	τ/τ_0§	τ_1 (s)	τ_2 (s)	τ_3 (s)	f_1	f_2	f_3
F_1 (3.5 μM)		1.0	1	4.92	1.61	0.34	0.6	0.26	0.14
F_1 + TNP-ATP	0.98	0.9 (0.96)	0.99	4.91	1.58	0.33	0.58	0.26	0.16
F_1 + TNP-ATP	2.5	0.87 (0.99)	0.99	4.87	1.6	0.32	0.61	0.24	0.15
F_1 + TNP-ATP	5.1	0.73 (1.0)	1.0	4.93	1.59	0.32	0.58	0.24	0.18
F_1 + TNP-ATP	10.1	0.44 (0.84)	0.9	4.42	1.47	0.3	0.6	0.25	0.15
F_1 + TNP-ATP	20.0	0.27 (0.81)	0.8	4.05	0.97	0.33	0.54	0.26	0.2
F_1 + TNP-ATP	52.0	0.047 (0.8)	0.78	3.97	0.93	0.36	0.55	0.27	0.18
F_1 + TNP-ATP + ATP	52.0	0.058 (0.97)	0.98	4.88	1.55	0.32	0.59	0.19	0.22
Trp (4 μM)		1.0	1.0	5.12		0.3	0.87		0.13
Trp (4 μM) + ATP (1 mM) + TNP-ATP (182 μM)		0.06 (1.01)	0.99	5.1		0.3	0.88		0.12

*Samples were in 50:50 (v/v) glycerol/buffer (20 mM MOPS, 10 mM KH_2PO_4, 2 mM $MgSO_4$, pH 7.4) at 180 K. For other details, see legend to Table 1.

#P/P_0 is the phosphorescence intensity ratio at 411 nm. In parentheses are values corrected for inner filter and trivial energy transfer using equimolar solutions of free Trp.

§τ and τ_0 refer to the average phosphorescence lifetime in the presence and absence of TNP-ATP, respectively, as given by $\tau = \alpha_1\tau_1 + \alpha_2\tau_2$ and $\alpha_1 = f_1/\tau_1(f_1/\tau_1 + f_2/\tau_2)$, etc.

third TNP-ATP molecule determined at ambient temperature (<0.5 μM). There are two possible explanations for this finding: either transfer occurs to TNP-ATP bound to a forth low-affinity site, or the above dissociation constant increases steeply at lower temperature. Binding isotherms are not accurately determined in glass media. However, at ambient temperature, under our experimental conditions, only three TNP-ATP molecules bind to the F_1 complex. Also, the K_D was shown to increase on lowering the temperature. Hence, we must conclude that the nucleotide binding affinity is drastically reduced in low-temperature glasses, and that energy transfer occurs selectively to the TNP-ATP molecule in the weakest catalytic site. Consequently, with respect to Trp in the ϵ-subunit, the TNP moiety is beyond the range of triplet-singlet energy transfer ($r \geq 6.4$ nm) when bound to the two higher affinity sites, whereas it is separated by about 4.9 nm when in the lowest affinity site.

Finally, it should be noted that because the donor–acceptor orientation is not known, distances were necessarily estimated assuming fixed and random orientation ($\kappa^2 = 0.476$). This assumption will introduce a degree of uncertainty on our distance determination, but it can be argued that the error cannot be unduly large. First, because both coumarin and TNP acceptor probes are joined by single bonds and are solvent exposed, they presumably enjoy a good degree of rotational freedom, and consequently, it is unlikely that they adopt a single dominant orientation. Inevitably some orientation will be more probable than others, and, strictly speaking, the complete randomness assumption would not apply. However, it is known that as more than one orientation becomes possible, the orientation factor approaches rapidly the random value, and the uncertainty in the distance determination is drastically reduced. In the case of OSCP-CPM the agreement in the distance obtained from fluorescence and phosphorescence energy transfer is quite significant in this respect, because it implies that on a 90° change in the direction of the donor transition dipole moment, the orientation factor remains quite similar. This result is plausible only if several orientations are permitted to the acceptor. At any rate, it should be pointed out that even an error as large as 50% on the orientation factor (κ^2) introduces merely a 7% error in the distance determination, an accuracy hardly required for the conclusions that are drawn from this study. For this reason the accuracy of distances determined in this study should not considered to be better than 10%.

DISCUSSION

The existence of a single copy of the ϵ peptide in F_1 allows fluorescence and phosphorescence resonance energy transfer techniques to investigate the spatial relationships between its lone Trp residue and specific sites in other subunits of the oligomer. This work estimates the distance between the indole side chain and chromophoric labels attached either to ATP bound to the catalytic sites of F_1 or to Cys-118 of the OSCP subunit complexed to F_1.

As discussed above, the ATP analogue TNP-ATP, under our experimental conditions, binds exclusively to the catalytic sites of F_1. Energy transfer results indicate that the TNP moiety in the two sites of higher affinity are out of the range of resonance energy transfer, a finding consistent with a separation between indole and TNP $\geq$6.4 nm. The weakest binding site is closer, and the donor-acceptor distance is estimated at 4.9 $\pm$ 0.5 nm. Mg-ATP itself exhibits a differential affinity for the three catalytic sites. However, Murataliev and Boyer (1994) have shown that, in the presence of magnesium, the order of affinity is altered relative to TNP-ATP, with the lowest affinity site for ATP becoming of highest affinity for TNP-ATP. Thus, with respect to Mg-

ATP, a high-affinity site is at about 4.9 nm, whereas the other two sites are beyond 6.4 nm from the ϵ subunit Trp.

Fluorescence and phosphorescence energy transfer from indole to the coumarin label attached to OSCP indicate that the interaction is effective only for the first molecule of OSCP-CPM bound to F_1 and yields a separation of 3.7 $\pm$ 0.5 nm between the chromophores. Furthermore, the observation that OSCP-CPM in excess of the molar ratio of 1:1 is out of the range of energy transfer ($r \geq 4.6$ nm) implies that the low-affinity sites described by Dupuis et al. (1985) are farther removed. Apparently, these weaker associations of OSCP to F_1 are not functionally relevant for conferring the oligomycin sensitivity to the enzyme, because F_1 complexed to stalk proteins containing a single copy of OSCP was fully competent (Collinson et al., 1994).

Plausible models of the subunit arrangement in mitochondrial F_1 rely heavily on available crystallographic structures but also on the results of cross-linking reactions and topological considerations based on the expected homology with other sources of the enzyme. Recent x-ray diffraction studies at a 0.28-nm resolution (Abrahams et al., 1994) have indicated that beef heart mitochondrial F_1 is a slightly flattened sphere 8 nm high and 10 nm across. The three α- and three β-subunits are arranged alternately like the segments of an orange around a central cavity occupied by the γ-subunit. The latter is arranged to form a coiled coil between two long α-helices along the vertical axis of pseudosymmetry. The helical structure reaches to about 1.5 nm from the top of the $\alpha_3\beta_3$ subassembly and protrudes about 3.0 nm from the bottom of the main body, in a stem that is almost certainly part of the 4.5-nm stalk in ATP-synthase. The nucleotide binding sites lie at the α- and β-subunit interface, in an equatorial plane roughly 4.7 nm from the top surface. The δ- and ϵ-subunits were not resolved in the crystallographic structure, but increased local variations in the electron density suggest that they are in the stem region. Cross-linking experiments (Baird and Hammes, 1977; Joshi and Burrows, 1990; Beharry and Bragg, 1989) have established that the ϵ- and γ-subunits are in contact with each other. Two possible regions of contact with the γ subunit are either at the top of the $\alpha_3\beta_3$ assembly, right into the dimple formed by the central cavity, or at its bottom, associated somewhere along the 3.0-nm stem protrusion (Fig. 4 *a*). However, geometrical considerations based on the distances determined in this study between ϵ and the catalytic sites indicate that the top location is most unlikely. First, it would entail a separation between the ϵ Trp and the nucleotide sites that is distinctly smaller than measured by energy transfer. Second, an ϵ subunit on top of the central cavity would be more symmetrically placed relative to the nucleotide sites than actually inferred from energy transfer. Assuming a globular shape for the ϵ-subunit, a sphere 2.2 nm in diameter (M_r 5000; specific volume, 0.73 g/cm^3) would fit rather tightly in the dimple at the top of the central cavity, and its position would be constrained along the axis of pseudosymmetry. As a result, the ϵ-subunit would be placed roughly equidistant from each nucleotide

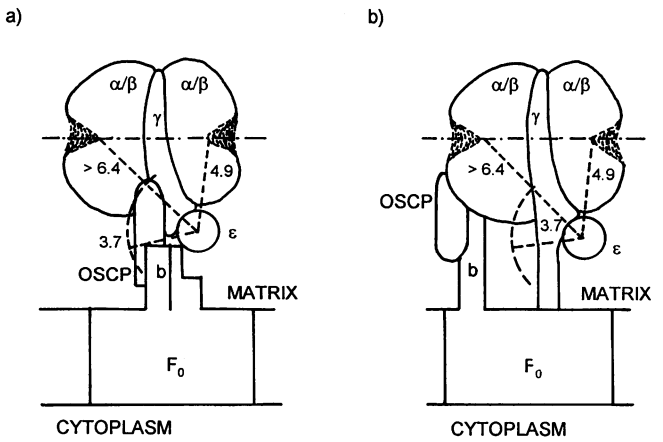

FIGURE 4 Two schematic representations of mitochondrial ATP-synthase: (*a*) as modified from Fig. 10 of Collinson et al. (1994), and (*b*) after the model of Duncan et al. (1995). The plausible location of the ϵ polypeptide (arbitrarily depicted as a *circle*) on the basis of the distances (nm) determined in this work is indicated. In (*a*) subunits b and OSCP are shown interacting with the stem region of F_1-ATPase, whereas in (*b*) they are shown interacting peripherally with the α- and β-subunits in accord with cross-linking data of Joshi and Burrows (1990) and Belogrudov et al. (1995).

site at a separation of 5.2 nm between its center and the TNP probe bound to the ribose ring of the nucleotide. According to the phosphorescence characteristics of Trp, the indole ring is buried inside the subunit (Solaini et al., 1993); therefore, it is likely to be near its center or not more than 0.5 nm from it. From these considerations the distance estimated between the Trp residue of the ϵ-subunit at the top of the cavity and the TNP chromophore in the catalytic sites is less than 5.7 nm. In this case each nucleotide would be within the 6.4-nm range of energy transfer, in contrast with the experimental observation that two of these sites are beyond this range. Furthermore, because the maximum displacement of the indole chromophore from the subunit center is about 0.5 nm, the smallest and largest distances with the nucleotide sites given by the most asymmetric arrangement of indole in the ϵ subunit would be 4.8 and 5.2 nm, respectively. This distance of 0.4 nm is distinctly less than 1.5 nm or more (between 4.9 and more than 6.4 nm) deduced experimentally. Thus, to be consistent with energy transfer, the ϵ-polypeptide must lie in the upper part of the stalk region of the F_1F_0 complex at a distance of 4.1 to 4.9 nm from the equatorial plane through the nucleotide binding sites (Fig. 4). Also, if as proposed by Abrahams et al., (1994) in the context of the binding change mechanism, catalytic action involves the rotation of $\alpha_3\beta_3$ around the pivot formed by the γ-subunit, then the finding that the ϵ subunit is always nearest to the lowest affinity TNP-ATP site requires that the small peptide be firmly attached to the γ central core and not be associated to the $\alpha_3\beta_3$ rotating frame.

It should be mentioned that the positioning of the ϵ-subunit also helps locate the δ-subunit, because evidence indicates that in mitochondrial F_1 the two smaller subunits are

closely associated (Baird and Hammes, 1977; Penin et al., 1990; Orriss et al., 1996).

It is interesting to note that the position of the ϵ-subunit derived here for mitochondrial F_1 is strikingly similar to the location of the ϵ-subunit in the chloroplast coupling factor, although sequence homology suggests that in the latter this polypeptide corresponds to the δ- rather than to the ϵ-subunit of the mitochondrial complex (Walker et al., 1985). Thus, in the chloroplast enzyme, the distances obtained from energy transfer between fluorescence labels attached to the sulfhydril of the ϵ-subunit and the TNP probe in the catalytic sites are 6.2 and 6.6 nm for the high-affinity sites and 4.9 nm for the low-affinity site. Also, the separation of ϵ from the membrane surface is 4.0 nm (Richter et al., 1985), which again is consistent with its location in the higher part of the stalk region.

Another important aspect of the F_0F_1 enzyme complex is the topological arrangement of the subunits linking the fragments F_0 and F_1. Presently, there are two models credited to represent the architecture of the F_0F_1 complex. In one (Fig. 4 *a*) F_1 is bound to the membrane sector through the central stalk that includes subunits b and OSCP, the pair, according to cross-linking data being closely associated with each other (Belogrudov et al., 1995; Joshi and Burrows, 1990). In the alternative model (Duncan et al., 1995) subunits b and OSCP connect the membrane domain by binding to one side of the F_1 globule (Fig. 4 *b*). The distance of 3.7 nm determined between the indole ring of the ϵ Trp and Cys-118 of OSCP places the two polypeptides in proximity, if not in direct contact, with each other. Indeed, assuming that they adopt a spherical shape, the molecular mass of 21,000 Da for OSCP yields molecular diameters of 3.6 nm, so that the maximum distance between indole and Cys-118 compatible with a contact complex is 5.3 nm; therefore, purely geometrical considerations cannot rule out a juxtaposition of the two polypeptides. Clearly, this proximity of ϵ to OSCP does not support the F_0F_1 model represented in Fig. 4 *b*, in which OSCP is placed at a considerable distance from the protruding stem of the γ-subunit. Furthermore, in the model of Fig. 4 *b*, OSCP and $\alpha_3\beta_3$ assembly have fixed positions relative to each other but not relative to the γ- or ϵ-subunit, which is firmly attached to it (see above). Hence, in the binding change mechanism the rotation of γ relative to $\alpha_3\beta_3$ would produce three equally probable but vastly different OSCP/ϵ-subunit spatial arrangements, each one characterized by a markedly different Trp4-Cys118 separation and, therefore, energy transfer efficiency. However, the agreement between the extent of energy transfer as determined by the decrease in phosphorescence intensity and by the reduction in phosphorescence lifetime implies homogeneous energy transfer efficiencies within the F_1 population, which in turn are consistent with a uniform OSCP/ϵ-subunit geometrical arrangement, as found in the model in Fig. 4 *a*.

We are grateful to Dr. J. E. Walker, and M. J. van Raaij (Medical Research Council, Cambridge, UK) for providing OSCP. We acknowledge the kindness of Prof. G. Lenaz (University of Bologna), in whose laboratory the enzyme was prepared.

This research was supported by Ministero dell'Università e della Ricerca Scientifica e Tecnologica (Rome) and by the Italian Consiglio Nazionale delle Ricerche.

REFERENCES

Abrahams, J. P., A. G. W. Leslie, R. Lutter, and J. E. Walker. 1994. Structure at 2.8 Å resolution of F_1-ATPase from bovine heart mitochondria. *Nature.* 370:621–628.

Abrahams, J. P., R. Lutter, R. J. Todd, M. J. van Raaij, A. G. W. Leslie, and J. E. Walker. 1993. Inherent asymmetry of the structure of F_1-ATPase from bovine heart mitochondria at 6.5 Å resolution. *EMBO J.* 12: 1775–1780.

Baird, B. A., and G. G. Hammes. 1977. Chemical cross-linking studies of beef heart mitochondrial coupling factor 1. *J. Biol. Chem.* 252: 4743–4748.

Baracca, A., M. Degli Esposti, G. Parenti-Castelli, and G. Solaini. 1992. Purification and characterization of adenosine triphosphatase from eel liver mitochondria. *Comp. Biochem. Physiol.* 101B:421–426.

Baracca, A., E. Gabellieri, S. Barogi, and G. Solaini. 1995. Conformational changes of the mitochondrial F_1-ATPase ϵ-subunit induced by nucleotide binding as observed by phosphorescence spectroscopy. *J. Biol. Chem.* 270:21845–21851.

Beharry, S., and P. D. Bragg. 1989. Conformational change in beef heart mitochondrial F_1 ATPase to ATP synthesis mode induced by dimethylsulfoxide and ATP revealed by sulfhydryl group labeling. *FEBS Lett.* 253:276–280.

Belogrudov, G. I., J. M. Tonich, and Y. Hatefi. 1995. ATP synthase complex. Proximities of subunits in bovine submitochondrial particles. *J. Biol. Chem.* 270:2053–2060.

Bianchet, M., S. Ysern, J. Hullihen, P. L. Pedersen, and L. M. Anzel. 1991. Mitochondrial ATP synthase. *J. Biol. Chem.* 266:21197–21201.

Boyer, P. D. 1989. A perspective of the binding change mechanism for ATP synthesis. *FASEB J.* 3:2164–2178.

Boyer, P. D. 1993. The binding change mechanism for ATP synthase: some probabilities and possibilities. *Biochim. Biophys. Acta.* 1140: 215–250.

Capaldi, R. A. 1995. F_1-ATPase in a spin. *Nature Struct. Biol.* 1:660–663.

Cioni, P., and G. B. Strambini. 1989. Dynamical structure of glutamate dehydrogenase as monitored by tryptophan phosphorescence. *J. Mol. Biol.* 207:237–247.

Collinson, I. R., M. J. van Raaij, M. J. Runswick, I. M. Fearnley, M. Skehel, G. L. Orriss, B. Miroux, and J. E. Walker. 1994. ATP synthase from bovine heart mitochondria. *J. Mol. Biol.* 242:408–421.

Cross, R. L., and C. M. Nalin. 1982. Adenine nucleotide binding sites on beef heart F_1-ATPase. *J. Biol. Chem.* 257:2874–2881.

Duncan, T. M., V. V. Bulygin, Y. Zhou, M. L. Hutcheon, and R. L. Cross. 1995. Rotation of subunits during catalysis by *Escherichia coli* F_1-ATPase. *Proc. Natl. Acad. Sci. USA.* 92:10964–10968.

Dupuis, A., J. Lunardi, J.-P. Issartel, and P. V. Vignais. 1985. Interactions between the oligomycin sensitivity conferring protein (OSCP) and beef heart mitochondrial F_1-ATPase. 1. Study of the binding parameters with a chemically radiolabeled OSCP. *Biochemistry.* 24:734–739.

Duszynsky, J., A. Dupuis, B. Lux, and P. V. Vignais. 1988. Spectral properties of fluorescent derivatives of the oligomycin sensitivity conferring protein and analysis of their interaction with the F_1 and F_0 sectors of the mitochondrial ATPase complex. *Biochemistry.* 27:6288–6296.

Eftink, M. R., and C. A. Ghiron. 1976. Exposure of tryptophan phosphorescence residues in proteins. Quantitative determination by fluorescence quenching studies. *Biochemistry.* 15:672–680.

Fernàndez-Moràn, H. 1962. Cell-membrane ultra-structure. Low temperature electron microscopy and X-ray diffraction studies of lipoprotein components in lamellar systems. *Circulation.* 26:1039–1065.

Förster, T. 1959. Transfer mechanisms of electronic excitation. *Discuss. Faraday Soc.* 27:7–17.

Galley, W. C., and L. Stryer. 1969. Triplet-singlet energy transfer in proteins. *Biochemistry.* 8:1831–1838.

Gresser, M. J., J. A. Myers, and P. D. Boyer. 1982. Catalytic site cooperativity of beef heart mitochondrial F_1 adenosine triphosphatase. *J. Biol. Chem.* 257:12030–12038.

Grubmeyer, C., and H. S. Penefsky. 1981. Presence of two hydrolytic sites on beef heart mitochondrial adenosine triphosphatase. *J. Biol. Chem.* 256:3718–3727.

Issartel, J. P., J. Lunardi, and P. V. Vignais. 1986. Characterization of exchangeable and nonexchangeable bound adenine nucleotides in F_1-ATPase from *Escherichia coli*. *J. Biol. Chem.* 261:895–901.

Joshi, S., and R. Burrows. 1990. ATP synthase complex from bovine heart mitochondria. *J. Biol. Chem.* 265:14518–14525.

Kellogg, R. E. 1967. Kinetics of energy transfer from the triplet state in rigid solutions. *J. Chem. Phys.* 47:3403–3406.

Laemmli, U. K. 1970. Cleavage of structural proteins during the assembly of the head of bacteriophage T_4. *Nature.* 227:680–685.

Lakowicz, J. R. 1983. Energy transfer. *In* Principles of Fluorescence Spectroscopy. Plenum Publishing Corp., New York. 303–339.

Lowry, O. H., N. J. Rosebrough, A. L. Farr, and R. J. Randall. 1951. Protein measurement with the Folin phenol reagent. *J. Biol. Chem.* 193:265–275.

McCarty R. E., and G. G. Hammes. 1987. Molecular architecture of chloroplast coupling factor 1. *Trends Biochem. Sci.* 12:234–237.

Muneyuki, E., T. Hisabori, W. S. Allison, J.-M. Jault, T. Sasayama, and M. Yoshida. 1994. Catalytic cooperativity of beef heart mitochondrial F_1-ATPase revealed by using 2′,3′-*O*-(2,4,6-trinitrophenyl)-ATP as a substrate; an indication of mutually activating catalytic sites. *Biochim. Biophys. Acta.* 1188:108–116.

Murataliev, M. B., and P. D. Boyer. 1994. Interaction of mitochondrial F_1-ATPase with trinitrophenyl derivatives of ATP and ADP. *J. Biol. Chem.* 269:15431–15439.

Orriss, G. L., M. J. Runswick, I. R. Collinson, B. Miroux, I. M. Fearnley, J. M. Skehel, and J. E. Walker. 1996. The δ- and ϵ-subunits of bovine F_1-ATPase interact to form a heterodimeric subcomplex. *Biochem. J.* 314:695–700.

Penefsky H. S. 1975. Preparation of beef heart mitochondrial ATPase. *Methods Enzymol.* LV:304–308.

Penefsky, H. S., and R. L. Cross. 1991. Structure and mechanism of F_1F_0-type ATP synthases and ATPases. *Adv. Enzymol.* 64:173–214

Penin, F., G. Deléage, D. Gagliardi, B. Roux, and D. C. Gautheron. 1990. Interaction between δ and ϵ subunits of F_1-ATPase from pig heart mitochondria. Circular dichroism and intrinsic fluorescence of purified and reconstituted $\delta\epsilon$ complex. *Biochemistry.* 29:9358–9364.

Richter, M. L., B. Snyder, R. E. McCarty, and G. G. Hammes. 1985. Binding stoichiometry and structural mapping of the ϵ polypeptide of chloroplast coupling factor 1. *Biochemistry.* 4:5755–5763.

Senior, A. E. 1988. ATP synthesis by oxidative phosphorylation. *Physiol. Rev.* 68:177–231.

Shapiro, A. B., K. D. Gibson, H. A. Scheraga, and R. E. McCarty. 1991. Fluorescence resonance energy transfer mapping of the fourth of six nucleotide-binding sites of chloroplast coupling factor 1. *J. Biol. Chem.* 266:17276–17285.

Solaini, G., A. Baracca, G. Parenti-Castelli, and G. B. Strambini. 1993. Tryptophan phosphorescence as a structural probe of mitochondrial F_1-ATPase ϵ-subunit. *Eur. J. Biochem.* 214:729–734.

Strambini, G. B. and M. Gonnelli. 1995. Tryptophan phosphorescence in fluid solution. *J. Am. Chem. Soc.* 117: 7646–7651.

Strambini, G. B., P. Cioni, A. Peracchi, and A. Mozzarelli. 1992. Characterization of tryptophan and coenzyme luminescence in tryptophan synthase from *Salmonella typhimurium*. *Biochemistry.* 31:7527–7434.

Stryer, L. 1968. Fluorescence spectroscopy of proteins. *Science.* 162: 526–533.

Tiedge, H., and G. Schäfer. 1986. Site-site interaction on mitochondrial F_1-ATPase. *Biol. Chem. Hoppe-Seyler.* 367:689–694.

Tzagoloff A., D. M. MacLennan, and K. H. Byington. 1968. Studies on the mitochondrial adenosine triphosphatase system. III. Isolation from the oligomycin-sensitive adenosine triphosphatase complex of the factors which bind F_1 and determine oligomycin sensitivity of bound F_1. *Biochemistry.* 7:1596–1602.

Walker, J. E., I. M. Fearnley, N. J. Gay, B. W. Gibson, F. D. Northrop, S. J. Powell, M. J. Runswick, M. Saraste, and V. L. J. Tybulewicz. 1985. Primary structure and subunit stoichiometry of ATPase from bovine mitochondria. *J. Mol. Biol.* 184:677–701.

Weber, J., and A. E. Senior. 1996. Binding and hydrolysis of TNP-ATP by *Escherichia coli* F_1-ATPase. *J. Biol. Chem.* 271:3474–3477.

Weber, J., S. Wilke-Mounts, R. S.-F. Lee, E. Grell, and A. E. Senior. 1993. Specific placement of tryptophan in the catalytic sites of *Escherichia coli* F_1-ATPase provides a direct probe of nucleotide binding: maximal ATP hydrolysis occurs with three sites occupied. *J. Biol. Chem.* 268: 20126–20133.